Paleobiology

www.cambridge.org/pab

Phylogenetic analyses reveal that horses deviate from a pervasive pattern of skull shape evolution

Anna L. Wisniewski[1,2] and Graham J. Slater[2]

[1]Museum of Paleontology, University of Michigan, Ann Arbor, Michigan 48109, U.S.A.
[2]Department of the Geophysical Sciences, University of Chicago, Chicago, Illinois 60637, U.S.A.

Article

Cite this article: Wisniewski, A. L., and G. J. Slater (2026). Phylogenetic analyses reveal that horses deviate from a pervasive pattern of skull shape evolution. *Paleobiology* **52**, 457–469.
https://doi.org/10.1017/pab.2026.10096

Received: 16 April 2025
Revised: 01 November 2025
Accepted: 15 January 2026

Handling Editor:
Celeste Pérez-Ben

Corresponding author:
Anna Wisniewski;
Email: annawis@umich.edu

Abstract

The mammalian skull plays important roles in sensing, communication, and obtaining and processing food. These diverse functions make the skull a natural target for investigating how developmental processes and selective pressures related to ecology interact to produce patterns of morphological evolution. Here, we investigate the evolution of the equid skull through the lens of craniofacial evolutionary allometry (CREA), a pattern of relative facial elongation in larger mammals that has been hypothesized to result from similar patterns of facial elongation over ontogeny. Using 3D geometric morphometrics and linear measurements, we describe the major axes of shape variation in the equid skull, test whether equids follow or deviate from the CREA pattern over the clade's evolutionary history, and assess whether the evolution of high-crowned teeth (hypsodonty) is related to relative facial proportions, all in an explicitly phylogenetic context. We find that equids deviate from the CREA pattern and that the evolution of hypsodont dentition did not significantly influence facial proportions in the group. Importantly, these results are only apparent when using statistics appropriate for phylogenetic data. Comparison with previously published data on facial proportions from modern equids indicates that ontogenetic patterns of facial elongation do not scale to produce patterns of facial proportions observed at the intraspecific and evolutionary levels. Taken together, our results complicate the historic narrative that a single set of selective factors drove patterns of morphological evolution within the group.

Non-technical Summary

The mammalian skull plays important roles in sensing, communicating, and obtaining and processing food, making it a useful model system to understand how developmental processes and selection for different ecological functions influence patterns of morphological evolution in general. Allometry describes changes in shape related to changes in size. Previous work has documented a pattern among mammals wherein larger species tend to have relatively longer faces than smaller species (craniofacial evolutionary allometry, or CREA). CREA mirrors patterns of skull shape change over postnatal development (ontogeny). Using 3D quantification of shape and linear measurements, we describe the major patterns of shape variation in equid (fossil and modern horses) skulls, test whether equids follow or deviate from the CREA pattern over the clade's evolutionary history, and identify whether the evolution of high-crowned teeth (hypsodonty) is related to relative facial proportions, all using statistics appropriate to evolutionary data. Those analyses demonstrate that fossil and modern horses do not conform to the CREA pattern and that the evolution of hypsodont dentition did not influence relative facial length in the group. Comparison with previously published data suggests patterns seen during growth do not necessarily scale up to explain evolutionary changes between species. Our results challenge the idea that a single developmental or ecological factor can fully explain skull evolution in horses.

© The Author(s), 2026. Published by Cambridge University Press on behalf of Paleontological Society. This is an Open Access article, distributed under the terms of the Creative Commons Attribution licence (http://creativecommons.org/licenses/by/4.0), which permits unrestricted re-use, distribution and reproduction, provided the original article is properly cited.

Introduction

Understanding the processes that generate patterns of morphological diversity is a fundamental challenge in evolutionary biology (Foote 1997; Jablonski 2017a, 2017b). Natural selection acts on standing phenotypic variation, and hypothetically, if no processes were to bias the production of phenotypic variation, morphological evolution could proceed in any number of directions. However, due to the nature of developmental systems, this is most often not the expectation (Jablonski 2020; Salazar-Ciudad 2021), and morphological evolution proceeds along constrained trajectories of shape covariation (Schluter 1996; Marroig and Cheverud 2005). One such set of trajectories describes changes in shape related to size. These scaling power laws can be evaluated at different levels of biological organization, and when analyzed across different species, these trajectories are known as evolutionary allometry (Klingenberg 2014).

Evolutionary allometry has recently received attention as a constraint on mammalian skull shape evolution (e.g., Cardini 2019; Marcy et al. 2020). Among closely related groups of mammals, facial length often increases proportionally more than braincase length as body size and total skull length increases (Radinsky 1985; Slater and Van Valkenburgh 2008; Cardini and Polly 2013; Cardini 2019; Rhoda et al. 2023; Tamagnini et al. 2023; but see Krone et al. 2019). When this occurs, larger species have relatively longer faces than smaller species in a pattern that was originally termed "progressive preoptic preponderance" (PPP; Robb 1935), and more recently has been called "craniofacial evolutionary allometry" (CREA; Cardini and Polly 2013; Cardini et al. 2015; Zelditch and Swiderski 2023). This evolutionary pattern seems to mirror the patterns seen in ontogeny (Cardini and Polly 2013); newborn mammals have relatively short or brachycephalic faces compared to adults, and over ontogeny, the face grows at a faster rate than the braincase, resulting in adults with longer or more dolichocephalic faces than juveniles (e.g., O'Higgins and Collard 2002; Gianni et al. 2010; Le Verger et al. 2020). If ontogenetic allometric trajectories form the basis for the CREA pattern, this would suggest that changes in adult morphology between species are achieved through changes in the timing of development (Gould 1985). However, the CREA pattern could also be due to the interaction between other allometric patterns and biomechanical constraints (Cardini and Polly 2013). For example, brain size, and by extension braincase size, scales with an exponent of 3/4 relative to body size (Martin et al. 2005). If jaw and facial lengths scale isometrically relative to body mass (an exponent of 1/3) (Emerson and Bramble 1993), then jaw and facial lengths would scale at a faster rate than braincase size, resulting in the CREA pattern (Cardini and Polly 2013).

Much of the early work on which PPP and CREA are based was focused on the rich fossil record of the horse family, Equidae (Robb 1935; Radinsky 1984). Over their ~55 million year evolutionary history, equids display a textbook set of trends toward larger size, loss of lateral digits, and increasingly large and high-crowned teeth, all of which are thought to associate with global trends toward a cooler climate, expansion of grasslands, and a shift from browsing to grazing diets (Janis 2007). Structural reorganization, due to the acquisition of high-crowned hypsodont teeth (Reeve and Murray 1942; Radinsky 1984), likely influenced patterns of evolutionary shape change in the equid skull. However, the degree to which allometry and hypsodonty drove skull shape variation has not yet been explicitly tested, beyond evaluating whether brachydont and hypsodont taxa differ in scaling proportions (Radinsky 1984). Furthermore, because all of these studies occurred before the comparative methods revolution of the mid-1980s, none considered the confounding effects of shared evolutionary history when analyzing evolutionary changes in equid skull morphology. More recently, facial length has been shown to scale isometrically (facial length scales at the same rate as braincase length) or with negative allometry (facial length increases at a slower rate than braincase length) in extant equids (Cardini 2019). Cardini (2019) hypothesized that this may be due to the spatial requirements of hypsodont dentition; large high-crowned teeth require more space, resulting in a proportionally longer rostrum even in smaller animals. In support of this idea, a recent analysis of modern horse and pony breeds found no evidence for craniofacial elongation in larger breeds, suggesting that despite artificial selection for small body size in miniature breeds, there are limits in the degree to which facial length can decrease while still maintaining adequate space in the palate for their dentition (Heck et al. 2019). However, evaluating the role hypsodonty played in shaping patterns of equid skull shape evolution requires the temporal perspective of the fossil record.

Here, using linear measurements, phylogenetic comparative methods, and the rich equid fossil record, we explicitly test whether equids follow or deviate from the CREA pattern and whether relative facial proportions are driven by hypsodonty. We then compare evolutionary patterns in relative facial proportions to those seen within species and over ontogeny. Finally, we use 3D geometric morphometrics to describe the major axes of shape variation in the equid skull and evaluate support for size and hypsodonty as drivers of shape variation in the equid skull.

Materials and Methods

The 2D and 3D Data

We collected 3D surface scan data for 31 skulls from 26 species of equid, spanning the family's entire evolutionary history (Table 1). We selected only adult specimens, with permanent adult dentition erupted. Our sample size is reflective of the availability of adequately preserved specimens for morphometric analysis. Skulls were scanned using a structured light scanner (Creaform Go! Scan 20) at 0.3 mm resolution. One scan (*Neohipparion affine* UNSM 101500), was downloaded from Morphosource (Morphosource Ark: ark:/87602/m4/475607; Goswami et al. 2022). To evaluate whether macroevolutionary patterns in equid skull evolution mirror those seen in ontogeny, we also collected a small ontogenetic sample of plains zebra (*Equus quagga*) totaling eight specimens ranging in age from late fetal/newborn to adult individuals (Supplementary Table S1). We quantified skull shape using a set of 18 landmarks, adapted from Heck et al. (2018, 2019; Fig. 1, Supplementary Table S2). For some specimens, where landmarks could not be placed due to lack of preservation or damage to the specimen, we estimated landmark position. To estimate the position of missing landmarks, we symmetrized, where possible, symmetric landmarks across a plane defined by midline (landmarks 15–18, Supplementary Table S2). For nonsymmetric landmarks, we estimated landmark position using the *fixLMtps* function in the Morpho R package (Schlager 2017). Estimated landmark configurations were checked via visual inspection to ensure that the resulting configuration appeared sensible. For one specimen, *Neohipparion affine* UNSM 101500, all missing landmarks were estimated using the *fixLMtps* function, because this resulted in the most reasonable estimates for bilaterally symmetric landmarks. Where possible, we landmarked two specimens per species. In these cases, we computed a species average landmark configuration using the *mshape* function in the geomorph R package (Baken et al. 2021; Adams et al. 2023). In analyses using 3D geometric morphometric data, it may be a concern when degrees of freedom ($3k + 7$, for 3D landmark data, where k is number of landmarks) exceed the number of specimens (Webster and Sheets 2010). To explore whether reducing the number of landmarks (and, therefore, degrees of freedom) impacted our results, we created an additional dataset in which we included only landmarks from the left side. We extracted the symmetric component of shape variation from the Procrustes-transformed full landmark dataset using the *bilat.symmetry* function in geomorph R package. We then discarded paired landmarks from the right side, such that only one half of the symmetric shape dataset was present (hereafter referred to as the "symmetric" dataset).

Facial length and braincase length were measured in two ways, following previous studies. Following Cardini (2019), we first calculated inter-landmark distances that defined the length of the face

https://doi.org/10.1017/pab.2026.10096 Published online by Cambridge University Press

Table 1. Evolutionary sample of equids included in the study.

Species	Specimen number	Scan data source
Cormohipparion occidentale	AMNH F:AM 71800	This paper
Dinohippus leidyanus	AMNH F:AM 87201	This paper
Equus (Amerhippus) andium	FMNH P 13671, FMNH P 14214	This paper
Equus asinus	USNM 252292, USNM 252293	This paper
Equus quagga	USNM 161930	This paper
Equus caballus	FMNH 57796	This paper
Equus (Dolichohippus) grevyi	USNM 163228, FMNH 26986	This paper
Equus (Hemionus) hemionus	USNM 521103	This paper
Equus (Asinus) kiang	USNM 084083, USNM A49493	This paper
Equus niobrarensis	USNM 12146	This paper
Equus przewalskii	USNM 238111, FMNH 57806	This paper
Equus scotti	FMNH P 12895	This paper
Equus zebra	USNM 270125	This paper
Haringtonhippus francisci	LACM 156450	This paper
Hyracotherium vasacciense	USNM PAL 336125	This paper
Megahippus matthewi	AMNH F:AM 60700	This paper
Merychippus insignis	AMNH 87001	This paper
Mesohippus bairdi	FMNH P 27240	This paper
Mesohippus exoletus	AMNH 74001	This paper
Mesohippus westoni	AMNH 74023	This paper
Miohippus obliquidens	F:AM 116328	This paper
Neohipparion affine	UNSM 101500	Goswami et al. 2022 (via Morphosource)
Parahippus cognatus	AMNH F:AM 71700	This paper
Pliohippus mirabilis	UNSM 1356	This paper
Pliohippus pernix	AMNH F:AM 60800	This paper
Scaphohippus intermontanus	AMNH 87301	This paper

as the distance between first incisors from ventral side (landmark 15) to the midpoint of the palate (landmark 16) and braincase length as the midpoint of the palate to the ventral tip of the foramen magnum (landmark 17) (Fig. 2, Supplementary Table S2). These landmarks reflect different developmental origins of the cranial elements, with the face deriving from the splanchnocranium and the braincase deriving from the neurocranium, and present reproducible points for landmark placement (Salamanca-Carreño et al. 2023; Cardini 2019; Hallgrímsson et al. 2006).

To mirror Radinsky's (1984) classic study of horse craniofacial allometry, we subsequently took linear measurements of toothrow length (= face length) from the posterior margin of M3 to the anterior margin of the incisors and braincase length from the paracondylar process to the back of the orbit from screenshots of the skulls in lateral view in Geomagic DesignX (3D Systems, North Carolina), which were exported as .png files. Measurements were taken in ImageJ. These measurements represent an alternative way of measuring the different facial components and, similarly to the Cardini measurements, reflect their different developmental origins (Radinsky 1984).

Finally, to expand our intraspecific and ontogenetic datasets and make direct comparisons with previously published studies, we collected inter-landmark distances corresponding to facial length and braincase length (i.e., the "Cardini measurements") from Heck et al. (2018, 2019). Our landmarks 15, 16, and 17, correspond to landmarks 37, 46, and 60, respectively, in the intraspecific dataset of Heck et al. (2018) and landmarks 37, 44, and 58, respectively, in the ontogenetic dataset of Heck et al. (2019). For the intraspecific sample of adult specimens from Heck et al. (2018), we analyzed the data from domestic horses, zebras, and donkeys separately. Heck et al. (2018) pooled data for donkeys and for zebras because of issues related to inconsistent species identification. Although the zebra and donkey data are "pseudointraspecific," we choose to include them here because they provide a useful point of comparison with the evolutionary, ontogenetic, and domestic breed data.

Retrodeformation of Hyracotherium vasacciense

In general, we excluded specimens that had been severely deformed due to taphonomic processes and were no longer symmetric. However, we were unable to obtain any suitably preserved hyracotheriine specimens. As we felt it was important to include at least one representative from the earliest equid subfamily, we retrodeformed one specimen of *Hyracotherium vasacciense* (USNM

https://doi.org/10.1017/pab.2026.10096 Published online by Cambridge University Press

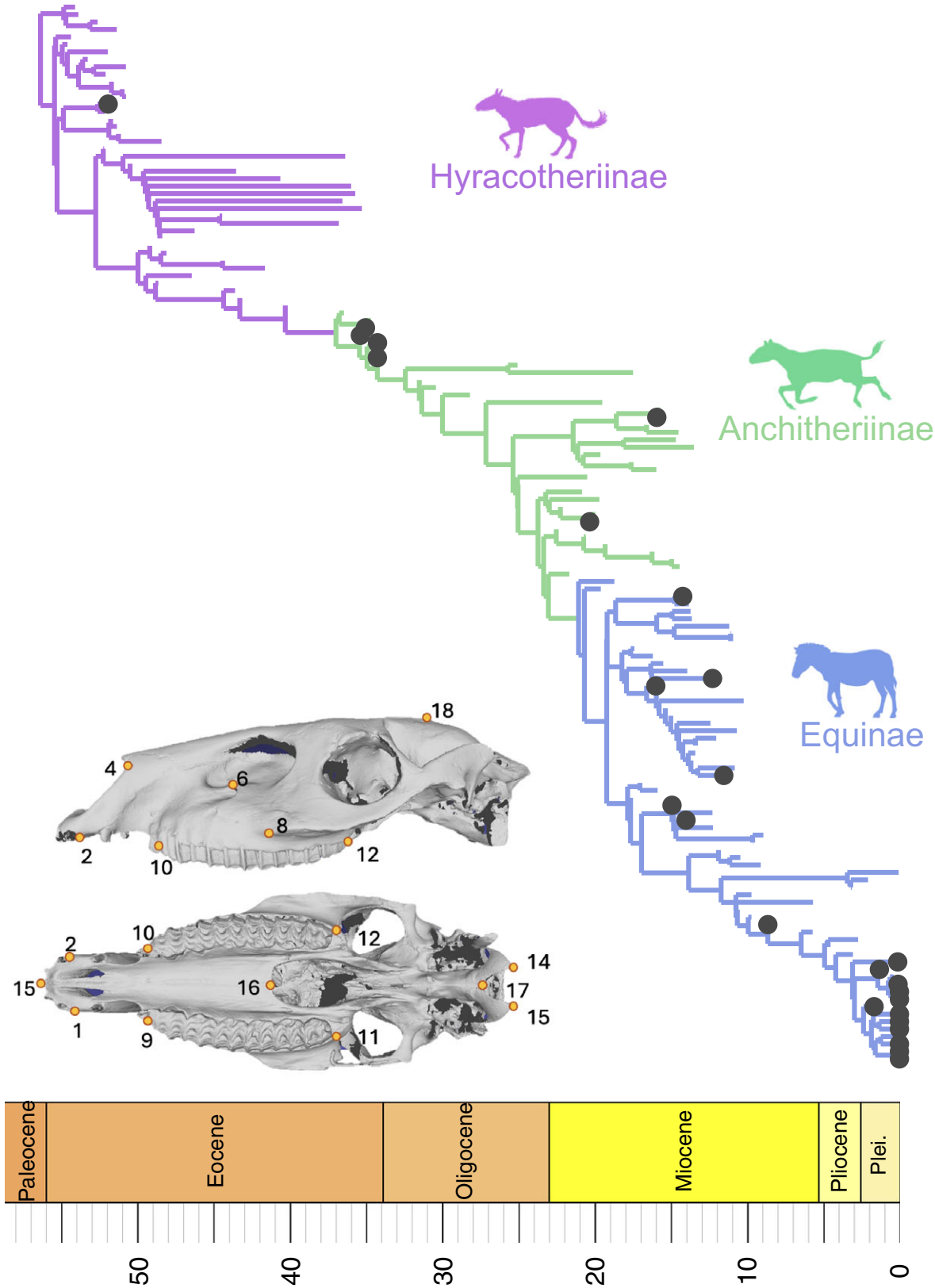


Figure 1. Median tree from BEAST2 v. 2.7.1 (Bouckaert et al. 2014) time-scaling analysis, with species represented in our dataset denoted by gray circular tips and skull of *Scaphohippus intermontanus* AMNH 87301 with landmark scheme; landmark descriptions can be found in Supplementary Table S2. Silhouettes are from phylopic.org donated under the CC0 1.0 Universal Public Domain Dedication license and Public Domain Mark 1.0 license.

https://doi.org/10.1017/pab.2026.10096 Published online by Cambridge University Press

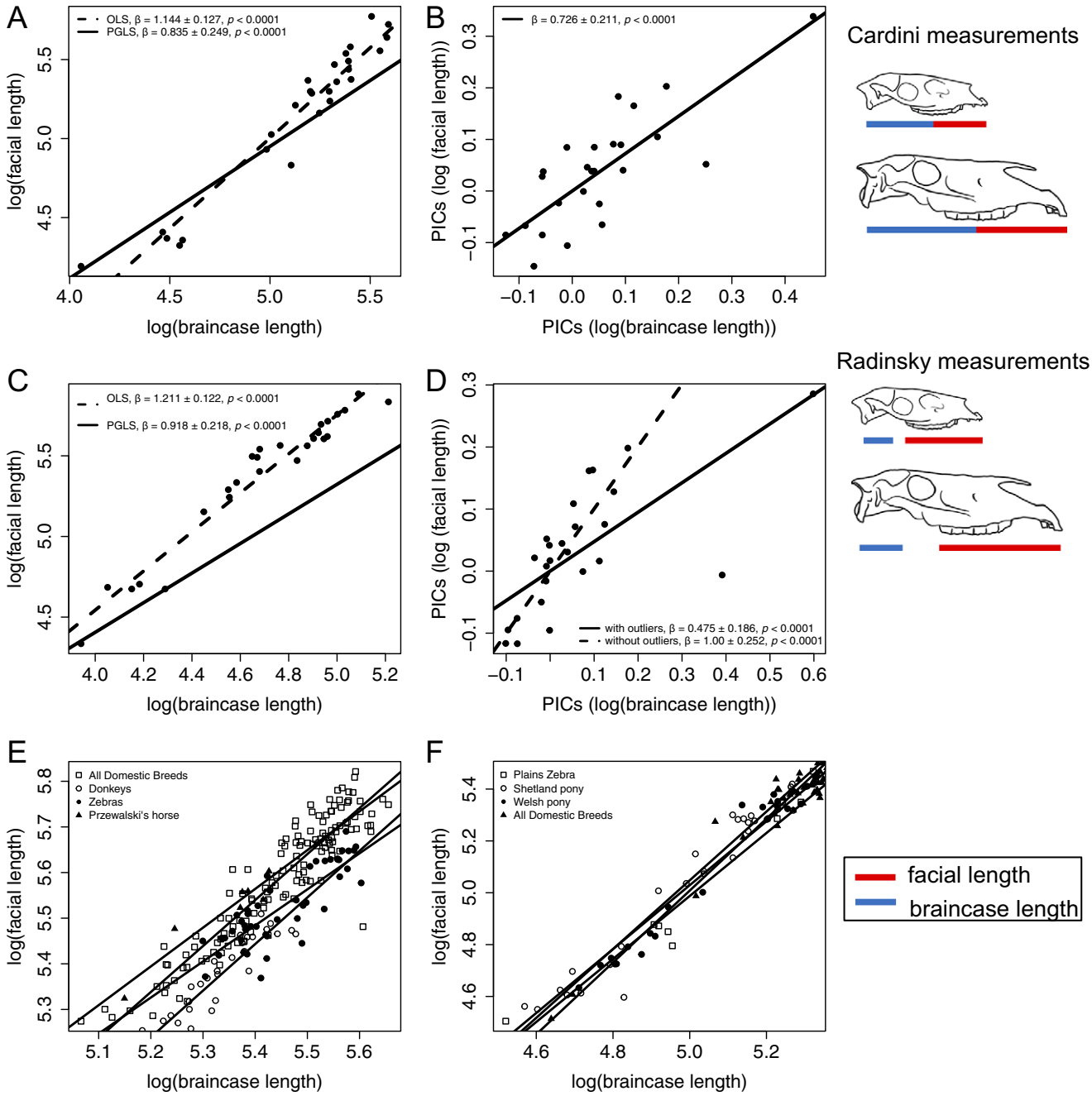


Figure 2. Examining craniofacial allometry across different levels of biological organization: **A, B,** use Cardini measurements of facial length and braincase length (Cardini 2019); **C, D,** use Radinsky measurements of facial length and braincase length (Radinsky 1984); **E, F,** use Cardini measurements. **A, C,** Regression of facial length onto braincase length shows that when phylogeny is taken into account, we cannot reject an isometric scaling relationship between facial length and braincase length, suggesting that equids deviate from the craniofacial evolutionary allometry (CREA) pattern. **E,** Regression of facial length onto braincase length shows that intraspecifically, among modern wild and domestic equids, facial length scales isometrically or with negative allometry relative to braincase length. **F,** Over ontogeny, equids follow CREA with facial length scaling with positive allometry relative to braincase length. Illustrations on the right-hand side denote the different measurement schemes for facial length and braincase length. OLS, ordinary least squares; PGLS, phylogenetic generalized least squares, PICs, phylogenetic independent contrasts.

PAL 336125) in which the rostrum and basicranium are slightly bent, using the method of Schlager et al. (2018).

This method works by placing landmarks and semilandmarks along bilaterally symmetric structures on the model. These landmarks are then symmetrized, and the deformed mesh is retrodeformed by thin plate spline deformation using the original and retrodeformed landmark coordinates (Schlager et al. 2018). We placed 104 landmarks (28 normal landmarks, 76 semilandmarks along curves) on the surface of the original model of USNM PAL 336125. We used the *slider3d* function in the R package Morpho (Schlager 2017) to slide semilandmarks along the curves. We then used the *symmetrize* function in Morpho (Schlager 2017) to create a symmetric landmark configuration; relaxed the original landmark configuration against the symmetric landmark configuration using the *relaxLM* function in Morpho (Schlager 2017); and used the resulting relaxed configuration to retrodeform the model of USNM

https://doi.org/10.1017/pab.2026.10096 Published online by Cambridge University Press

PAL 336125 with the *retroDeformMesh* function in the R package Morpho (Schlager 2017). Success of the retrodeformation process was assessed via visual inspection (Supplementary Fig. S1). We then landmarked the retrodeformed model using the original landmark configuration (Supplementary Fig. S1, Supplementary Table S2).

Metatree

Comparative evolutionary analyses require a time-scaled phylogeny to account for covariation due to shared ancestry among traits (Felsenstein 1985; Grafen 1989). However, a time-scaled phylogeny that incorporates most species in family Equidae does not yet exist, beyond informally constructed supertrees (e.g., Mihlbachler et al. 2011; Famoso et al. 2016; Cantalapiedra et al. 2017; Parker et al. 2018). These trees rely on qualitative assumptions about phylogenetic affinity of individual taxa and cannot explicitly incorporate uncertainty inherent in phylogenetic datasets.

Here, we employed the metatree approach (Lloyd et al. 2016; Lloyd and Slater 2021; Wisniewski et al. 2022) to generate a comprehensive, time-scaled, consensus evolutionary hypothesis for living and fossil equids. A metatree is a meta-analytic phylogeny that uses matrix representation with parsimony (MRP; Baum 1992; Ragan 1992a, 1992b) to summarize current consensus regarding relationships within a focal clade. Unlike typical MRP supertrees that encode only a single figured topology and weight each MRP character equally, metatree uses reanalysis of published phylogenetic matrices to obtain and encode all bipartitions of taxa present in the complete set of most parsimonious trees (MPTs) and summarizes the resulting phylogenetic information using a formal set of weighting rules to account for synonymy, composite terminal taxa, matrix reuse, year of publication, and MRP dataset size. For a detailed description of the analytic pipeline, we refer readers to Lloyd and Slater (2021). For this study, we sourced 16 morphological character–taxon matrices from 15 previously published studies (1 study had two matrices; Table 2). Following the metatree pipeline, we reanalyzed each of the morphological character–taxon matrices in TNT v. 1.6 (Goloboff and Morales 2023) under the original character ordering and weighting schemes (parameters for each search are provided in the analysis files, see Dryad Repository (https://doi.org/10.5061/dryad.crjdfn3g3) and summarized the resulting phylogenetic information from each analysis in MRP matrices. As molecular sequence information is also phylogenetically informative for extant and recently extinct species, we also generated an MRP representation of the maximum clade credibility (MCC) tree resulting from a BEAST v. 1.8.4 (Drummond et al. 2012) analysis of mitochondrial dataset 5 (filename=filename=BEAST_mtDNADataset5_equidsOnly_allPartns_rootConstrained_inclEovodovi.mcc) from Heintzman et al. (2017). This molecular phylogeny includes multiple tips per species and so, before generating the MRP matrix, we pruned the topology so each species was represented by one specimen. We used the *Metatree* function in the metatree R package (Lloyd 2015) to generate a global MRP matrix that summarized phylogenetic information across studies, while reconciling taxonomy using the Paleobiology Database (PBDB, https://paleobiodb.org). At this point, species with identical MRP coding were removed via safe taxonomic reduction to reduce noise and improve tree search efficiency. We analyzed the global MRP matrix in TNT v. 1.6 (Goloboff and Morales 2023) using 10,000 replicates, which resulted in 3774 MPTs. Species removed via safe taxonomic reduction were reinserted and a majority rule consensus (MRC) tree generated.

Table 2. Source studies used in metatree.

Citation	Type
Heintzman et al. 2017	Molecular
Bai et al. 2018	Morphological
Barrón-Ortiz et al. 2019	Morphological
Bennett 1980	Morphological
Cirilli et al. 2021	Morphological
Danilo et al. 2013	Morphological
Evander 1989	Morphological
Froehlich 2002	Morphological
Hulbert 1989	Morphological
Hulbert and MacFadden 1991	Morphological
Kelly 1998	Morphological
O'Sullivan 2002	Morphological
Pagnac 2006	Morphological
Prado and Alberdi 1996	Morphological
Rose et al. 2014	Morphological
Woodburne 2007	Morphological

To time-scale the topology for downstream analyses, we inferred branch lengths under a relaxed molecular clock and fossilized birth–death tree prior using BEAST2 v. 2.7.1 (Bouckaert et al. 2014). We used the MRC tree as a topology constraint, stratigraphic data from the PBDB as priors on the occurrence times for fossil taxa, and consensus sequence data derived from the molecular alignment of Heintzman et al. (2017) for estimating molecular branch lengths under the original partitions and models of molecular evolution. Three species for which we collected surface scan data, but which were not represented in the phylogenetic data (*Mesohippus exoletus*, *Mesohippus westoni*, and *Parahippus cognatus*), as well as a handful of other species that were relevant to future projects using the phylogeny, were manually inserted into the phylogeny based on taxonomy and topologically constrained via a series of "MRCA with rogues" priors that allowed the phylogenetic placement of these species to be resolved based on stratigraphic data.

The fossilized birth–death process (Heath et al. 2014; Gavryushkina et al. 2017) was used as a tree prior (net diversification rate prior, r ~exponential[1.0]; origin, ϵ ~exponential [2.301761], offset 56; fossil sampling probability prior, s ~β[2, 2]; turnover prior, ϵ ~β[2,1]), with an optimized relaxed lognormal clock model (mean = −4.24, SD = 1.25). We ran four Markov chain Monte Carlo chains of 100 million generations, sampling every 500,000 replicates. We extracted the median tree using the *medTree* function in the treespace R package (Jombart et al. 2017) to use as a phylogenetic framework for downstream analyses. Before analyses, we added 0.01 Myr to all zero-length branches (i.e., sampled ancestors).

Tests of Allometry

We first reevaluated the CREA hypothesis, that is, that facial length scales with positive allometry relative to braincase length, by performing phylogenetic regressions of ln(facial length) on ln(braincase length) for 26 species of living and extinct equids, spanning ~55 Myr of evolutionary history, using the median tree

https://doi.org/10.1017/pab.2026.10096 Published online by Cambridge University Press

from our BEAST2 v. 2.7.1 (Bouckaert et al. 2014) analysis as our main phylogenetic framework (Fig. 1). We fit phylogenetic generalized least squares (PGLS) regressions in R with lambda co-estimated.

We interpreted a 95% confidence interval for the slope that is greater than 1 to represent positive allometry, a 95% confidence interval that includes 1 as failure to reject isometry (the null model), and a 95% confidence interval that is less than 1 as evidence for negative allometry of facial length. For the purposes of comparison with previously published work (Radinsky 1984) we also fit ordinary least squares (OLS) and reduced major axis (RMA) regressions and performed analyses for two different sets of facial and braincase length measurements (based on measurements from two previous studies by Radinsky [1984] and Cardini [2019]; Fig. 2).

Statistical analyses were conducted using the *lm*, *gls*, and *lmodel2* functions in the stats, nlme, and lmodel2 R packages, respectively. Regressions were performed with both Cardini and Radinsky measurements. To test whether variation in phylogenetic tree structure had a tangible influence on the results of the phylogenetic regressions, we conducted PGLS regressions using a random sample of 100 trees from the posterior distribution. To test allometric patterns of facial elongation at the intraspecific level and ontogenetic level, we fit OLS regressions of facial length onto braincase length.

Influence of Acquisition of Hypsodont Dentition

To test whether the acquisition of hypsodont dentition influenced patterns of relative facial elongation, we fit OLS and PGLS regressions natural-log (ln)-transformed relative facial length (facial length/braincase length) onto an ln-transformed hypsodonty index. Hypsodonty index data were taken from Cantalapiedra et al. (2017) and Parker et al. (2018).

Axes of Shape Variation in the Equid Skull

It is possible that the simple measures of face and braincase length that we used earlier, following previous workers, fail to accurately describe overall patterns of craniofacial shape variation and therefore miss CREA-like patterns. To investigate the evolution of equid skull shape in a more holistic fashion, after performing a generalized Procrustes analysis on the landmark data to remove variation not due to shape (i.e., translation, rotational, and scaling effects; Goswami and Polly 2010), we performed a principal components analysis (PCA) of the shape data to explore the major axes of shape variation in the equid skull. We then created deformation grids using the *plotRefToTarget* function in the geomorph R package (Adams and Otárola-Castillo 2013). To investigate the relative contributions of hypsodonty, size, and first appearance data on skull shape variation we performed a series of multivariate phylogenetic least squares regressions using the *mvgls* function in the mvMORPH R package (Clavel et al. 2015).

Results

CREA and Evolutionary Allometry

Although OLS and RMA regressions were consistent with the predictions of CREA (OLS: Cardini measurements 95% confidence interval [CI] $\beta = 1.09-1.33$; Radinsky measurements 95% CI, $\beta = 1.02-1.27$; Supplementary Tables S3, S4), appropriately accounting for phylogenetic autocorrelation in the residual error of the model yields point estimates for the slope consistent with negative allometry (Fig. 2A,C, Supplementary Tables S3, S4), although isometry cannot be rejected because the 95% confidence intervals encompass 1 (Cardini measurements, $\beta = 0.83 \pm 0.25$, $p < 0.0001$; Radinsky measurements, $\beta = 0.92 \pm 0.22$, $p < 0.0001$). This result is insensitive to the choice of measurement dataset (Cardini measurements, $\beta = 0.83 \pm 0.25$, $p < 0.0001$; Radinsky measurements, $\beta = 0.92 \pm 0.22$, $p < 0.0001$), variation in tree topology (Fig. 3), use of phylogenetic independent contrasts (Fig. 2B,D), or use of phylogenetic reduced major axis regression (Cardini measurements, $p = 0.34$; Radinsky measurements $p = 0.62$). Taken together, these results indicate that phylogenetic autocorrelation inflates the signal for the CREA pattern in comparative data and confirms that evolutionary isometry of facial length cannot be rejected for equids.

Static and Ontogenetic Allometry

As with the evolutionary sample, equids deviate from the predictions of CREA at the intraspecific/"pseudointraspecific" level (Fig. 2E, Supplementary Table S5). In Heck et al.'s (2018) intraspecific sample of domestic horse breeds, donkeys, zebras, and Przewalski's horses (*Equus przewalskii*), facial length scales isometrically or with negative allometry with braincase length ($\beta_{horse} = 1.01 \pm 0.07$, $p < 0.001$; $\beta_{donkey} = 1.02 \pm 0.12$, $p < 0.001$; $\beta_{zebra} = 0.79 \pm 0.15$, $p < 0.001$; $\beta_{Prze.horse} = 0.85 \pm 0.32$, $p = 0.001$; Supplementary Table S5).

In contrast, facial length scales with positive allometry relative to braincase length over ontogeny in modern equids (Supplementary Table S6). Regression of facial length onto braincase length yields estimates for the slope that are universally greater than 1 and, in all cases except a small zebra sample that we collected for this study, have confidence intervals that only encompass values greater than 1 (Supplementary Table S6). Shetland and Welsh breeds have slightly larger estimates for the slopes than the sample of all domestic breeds and the sample of plains zebra. A PCA of the ontogenetic shape data for plains zebra suggests that increases in facial length relative to braincase length are a major axis of shape variation

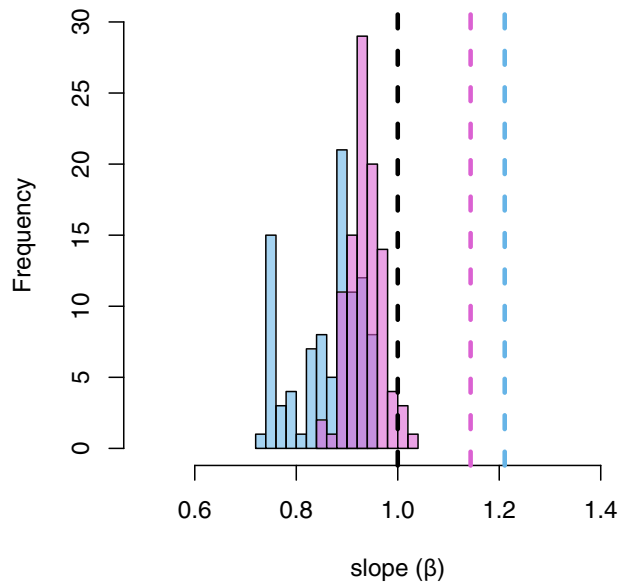


Figure 3. Distribution of point estimates for slope from phylogenetic regression of facial length onto braincase length across distribution of 100 randomly sampled trees. Black line denotes slope = 1. Pink and blue lines denote non-phylogenetic ordinary least squares (OLS) estimate for slope of regression of facial length onto braincase length using Cardini and Radinsky measurements respectively (Radinsky 1984; Cardini 2019).

https://doi.org/10.1017/pab.2026.10096 Published online by Cambridge University Press

(Supplementary Fig. S3). PC 1 explains 56.74% of shape variation in the sample and tends to separate older specimens (negative loadings) from younger specimens (positive loadings). Inspection of warped meshes representing shape changes associated with minimum and maximum scores on PC 1 shows that shape changes along this axis are driven in part by facial lengthening. This is most apparent in the diastema between the incisors and post-canine dentition where older specimens have a relatively longer diastema than younger specimens.

Axes of Shape Variation in the Equid Skull

PC 1, which explains 58.71% of the variance, defines changes in shape that qualitatively appear to be related to facial elongation—taxa that appear to have shorter rostra, such as *Hyracotherium*, have negative scores on PC 1 while taxa that appear to have elongate rostra, such as fossil and modern *Equus*, fall on the positive end (Fig. 4). Careful inspection of deformation grids that describe global and local patterns of shape change along PC 1 reveals that this apparent pattern is somewhat of an optical illusion (Fig. 4). Rather than reflecting elongation of the face, relative to the braincase, the first principal axis of shape variation in equids relates primarily to shearing of the skull along an antero-posterior axis, with more positive scores on PC 1 associated with retraction of the anterior tips of the dorsally placed nasal bones (landmarks 3 and 4; Supplementary Table S3, Fig. 4) and posterior displacement of the infraorbital foramen, combined with anterior displacement of the more ventrally placed facial crest (landmarks 5 and 6; Supplementary Table S3; Fig. 4). These shape changes mirror those observed in form space (shape + size; Supplementary Fig. S2).

Using phylogenetic multivariate regressions, we find that size is not a significant predictor of multivariate shape (Supplementary Tables S7, S8). These results are fairly consistent regardless of differences in tree topology and branch lengths, with 99–100% of trees yielding a nonsignificant relationship between full multivariate shape and size (Supplementary Table S9). We also find little evidence that the acquisition of hypsodont dentition influenced equid skull shape over the group's evolutionary history. Phylogenetic regression of multivariate shape onto hypsodonty index (Supplementary Table S7, Supplementary Table S8, $p > 0.05$ for 96–100% of trees) and relative facial length onto hypsodonty index (Fig. 5, Supplementary Tables S10, S11) indicate a nonsignificant relationship between these variables.

Inspection of Figure 4 also suggests that position on PC 1 is related to species age, with older species loading more negatively and more recent species loading more positively. However, we find it is not a significant predictor of multivariate shape regardless of tree topology or underlying dataset (Supplementary Tables S7–S9).

Discussion

A dominant theme in evolutionary biology is uniting patterns of morphological evolution observed in nature and the fossil record with the processes that generated them. One approach to this synthesis is to investigate evolutionary trends, that is, a consistent directional trajectory in phenotypic evolution, and test the developmental, environmental, or phylogenetic factors underlying them (Tamagnini et al. 2021). One such evolutionary trend is craniofacial evolutionary allometry (CREA), or the tendency for larger species of mammals to have relatively longer faces than smaller species (Cardini and Polly 2013; Tamagnini et al. 2017; Cardini 2019), with few exceptions (Richardson et al. 2024). CREA has also been tested in other non-mammalian groups such as synapsids (Krone et al. 2019) and birds (Bright et al. 2016; Linde-Medina 2016) with some support, suggesting that the trend could apply to amniotes as a whole. Changes in the timing of development have been suggested as a driver of the CREA pattern based on the observation that newborn animals tend to have relatively shorter faces than adults, and over ontogeny, the face grows at a faster rate than the braincase, resulting in a positive ontogenetic allometric trajectory (Wayne 1986).

We find, however, that when appropriate statistical tests are applied, we cannot reject an isometric scaling relationship between facial length and braincase length over equid evolutionary history. Point estimates of the scaling relationship between facial length and braincase length, as well as comparison of rates of evolution of facial length and braincase length, instead indicate isometry or negative craniofacial allometry. Our results are insensitive to how facial length and braincase length are measured or phylogenetic uncertainty, and indicate that equids present an exception to the CREA "rule" (Cardini 2019).

On the Importance of Phylogenetic Comparative Methods for Studying Evolutionary Allometry

Although the need to account for phylogenetic autocorrelation in the residual error term of evolutionary regressions should, today, be uncontroversial, it remains a bone of contention among comparative paleobiologists. The classic studies of horse craniofacial evolution that gave rise to the CREA hypothesis (Robb 1935; Reeve and Murray 1942; Radinsky 1984) predated the origin of phylogenetic comparative methods (Felsenstein 1985), in some cases by decades, but more recent authors continue to debate the need for their use. Recently, it has been argued that the use of phylogenetic regression might "erase" the signal for allometric scaling relationships in evolutionary regressions if size changes in a concerted fashion over a group's evolutionary history (Mitchell et al. 2024).

This logic was followed by Richardson et al. (2024), who used it as a reason to analyze the evolution of CREA in kangaroos using non-phylogenetic methods. However, this misunderstanding reflects common misconceptions about PGLS regression (Symonds and Blomberg 2014). OLS regression assumes that residual errors are identical and independently distributed, an assumption that may be violated by evolutionary data, because closely related species are expected to be more similar to one another than either is to more distantly related species and, hence, are also expected to have more similar residual errors. PGLS accounts for this autocorrelation by scaling the residual error term in the model by the (transformed) phylogenetic covariance matrix. Importantly, phylogenetic signal in the traits themselves may or may not translate to phylogenetic signal in the residual error term (Revell 2010). As a result, the only appropriate ways to test for CREA are either to first evaluate phylogenetic signal in the residual error term of the model and then to choose the appropriate phylogenetic or non-phylogenetic approach (Uyeda et al. 2018) or to co-estimate phylogenetic signal with the regression parameters (Revell 2010).

Concerns that PGLS may fail to detect a true allometric scaling relationship when the predictor covaries with phylogeny are easily ameliorated. To demonstrate this, we first simulated two traits evolving in a correlated fashion (e.g., an allometric scaling relationship between size and shape) on our equid tree using the *mvSIM* function in the mvMORPH R package (Clavel et al. 2015; Supplementary Fig. S4). As expected, PGLS consistently

https://doi.org/10.1017/pab.2026.10096 Published online by Cambridge University Press

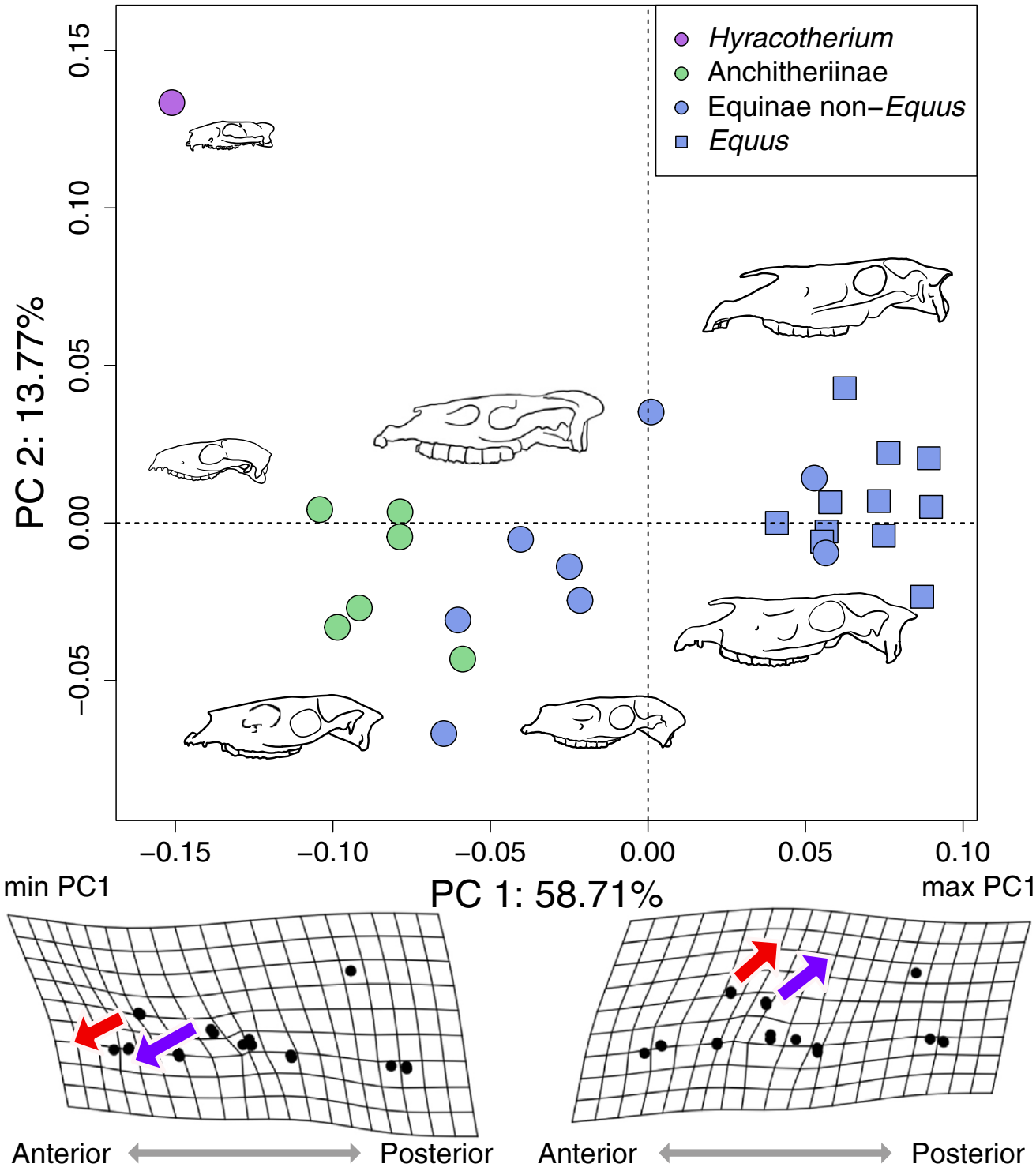


Figure 4. Visual inspection of a principal components analysis (PCA) of the shape data indicates phylogenetic, temporal, and size trends in skull shape. Larger, more recent species load more positively on PC 1, and older smaller species load more negatively on PC 1. However, larger species do not have proportionally longer faces based on phylogenetic regressions and regression of PICs (phylogenetic independent contrasts) of facial length onto braincase length (Fig. 2A–D). Deformation grids representing shape change associated with negative and positive scores along PC 1. Landmarks at nasals (3, 4) and infraorbital foramen (5, 6) are denoted with red and purple arrows, respectively, to emphasize changes in the position of the landmarks across PC 1. Outlines represent *Hyracotherium vasacciense*, *Equus przewalskii*, *Dinohippus leidyanus*, *Scaphohippus intermontanus*, *Megahippus matthewi*, and *Mesohippus exoletus*.

recovers a significant positive relationship between values (Supplementary Fig. S4A,B; see also Revell 2010). More significantly, though, PGLS can appropriately discriminate between two traits evolving under uncorrelated and correlated trends, while OLS struggles to discriminate between these scenarios (Supplementary Fig. S4C–F). These findings demonstrate that evolutionary patterns may be consistent with multiple generating processes (and vice versa; Raup and Gould 1974) and can

https://doi.org/10.1017/pab.2026.10096 Published online by Cambridge University Press

only be disentangled with knowledge of the underlying structure of the evolutionary tree (Foote et al. 1996).

Patterns of Facial Allometry across Levels of Biological Organization

One putative explanation for the CREA pattern in mammals is that allometric variation at the intra- and interspecific levels (i.e., static and evolutionary allometry) mirrors patterns of size-related variation that emerge through development (ontogenetic allometry) (Robb 1935). Although positive allometry of the facial skeleton, relative to the braincase, is apparent in ontogenetic samples of both domestic breeds and a small sample of wild-collected plains zebra, analyses of equid craniofacial allometry at the intraspecific level show that, among both domestic and wild extant taxa, facial length scales either isometrically or with negative allometry relative to braincase length. Artificial selection to produce different domestic breeds of horse serves as an analogue system to natural selection, although operating over much shorter timescales and with possibly different evolutionary potential in terms of standing genetic and phenotypic variation. Here, though, we find that patterns of craniofacial isometry mirror each other between the evolutionary level on the one hand and the intraspecific level within domestic horse breeds of drastically different body size (replicating the work of Heck et al. [2019]) and wild equid populations on the other. This suggests that this isometric scaling relationship was established early and conserved within the evolutionary history of this group. Whether a deviation from CREA is unique to equids or has deeper or repeated evolutionary origins in eutherian mammals has yet to be answered. Rhoda et al. (2023) recently found strong support for CREA acting as an evolutionary line of least resistance within ruminant artiodactyls, which would suggest that craniofacial adaptations to herbivory and ungulate ancestry alone are not drivers of this pattern. However, tests within other perissodactyl clades, both extant (rhinos and tapirs) and extinct (e.g., brontotheres) would also be informative.

Drivers or Correlates of Equid Craniofacial Shape Evolution

It has been suggested that the acquisition of specialized dentition may result in a deviation from established allometric patterns in mammals (Slater and Van Valkenburgh 2008; Cardini 2019; Heck et al. 2019; Tamagnini et al. 2023). For example, Meloro and Slater (2012) found rostrum shape was largely determined by canine height in sabertooth cats, while rostrum shape in non-sabertooth cats was largely driven by allometry. However, evolutionary covariation between the rostrum and braincase remained strong in both groups due to the biomechanical need to maintain structural cohesion within the skull.

The prediction that hypsodont dentition influenced relative facial proportions had been suggested for fossil and modern equids, but never tested with modern phylogenetic statistics (Robb 1935; Reeve and Murray 1942; Radinsky 1984). Here, we find that size is not significantly associated with multivariate shape variation in the equid skull (Supplementary Tables S8, S9), and there is no significant association between relative facial length and hypsodonty index (Fig. 5, Supplementary Tables S10, S11). Together, these results suggest that the evolution of hypsodont dentition did not play a significant role in driving skull shape evolution in equids.

If not the acquisition of hypsodont dentition or evolution along the CREA line of least resistance, what factors did drive equid skull evolution? It is worth noting here that not every trait needs to have a

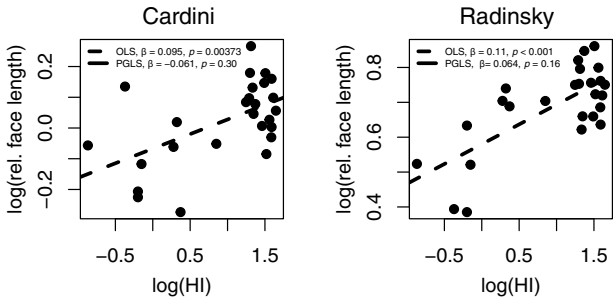


Figure 5. Phylogenetic regression of relative facial length onto hypsodonty index (HI) reveals that hypsodonty index does not predict facial proportions in equids. OLS, ordinary least squares; PGLS, phylogenetic generalized least squares. Cardini and Radinsky measurements derived from Cardini (2019) and Radinsky (1984), respectively.

single adaptive origin (Gould and Lewontin 1979). The skull is involved in many competing functions, including acquisition and processing of food, housing of sensory organs, and communication. These competing demands all likely constrained skull shape evolution within the equids to a limited number of directions, even with the acquisition of novel morphologies like hypsodont dentition (Bibi and Tyler 2022). Furthermore, because of the nature of geometric morphometric data, we are only able to analyze here the aspects of shape captured by homologous landmarks and thus miss, for example, the complex facial fossae that are found in many ancient equids, but which are absent in modern taxa (e.g., Fig. 1). These fossae are taxonomically diagnostic and may have been important for visual, auditory, and chemical communication and species recognition (Janis 2007). For example, Gregory (1920; cited in MacFadden and Skinner 1982) suggested that the dorsal preorbital fossa housed an expanded nasal diverticulum, a blind pocket located dorsally within each nostril (Budras et al. 2012), which helps form vocal signals such as snorts (Janis 2007).

Evidence from modern horses also indicates that the region of the dorsal preorbital fossa serves as the site of origination for the m. levator labii superioris muscle that inserts on the upper lip (Budras et al. 2012) and therefore serves critical functions in both visual signaling via lip elevation, as well as the "Flehman" response that allows pheromones, hormones, and scent to be transmitted to the vomeronasal organ (Estes 1972; Crowell-Davis and Houpt 1985; Janis 2007). Modern equids also use their lips extensively to acquire and manipulate food, and it is possible that a more robust m. levator labii superioris was selectively advantageous, particularly among browsing and mixed feeding equids.

Fossil and modern horses have long served as a hallmark example of evolution in the fossil record and were instrumental in developing macroevolutionary theory (Simpson 1944, 1953; Hansen 1997). One of the reasons the equids are such an appealing model system is that they display several obvious concerted changes in morphology, including increases in body size, acquisition of hypsodont dentition, and reduction of digits (MacFadden 1994). It is tempting to assume these changes evolved in response to a single set of selective pressures, such as the transition from closed habitats to open habitats over the Cenozoic (Wing 1998; Strömberg 2006), and that, as a result, we would observe integrated changes in morphology as the result of shifts in ecology. However, our results show that changes in craniodental morphology that appear to happen in a concerted fashion are actually decoupled over equid evolutionary history—the trend toward increased size and the associated changes in equid skull shape are not related to

https://doi.org/10.1017/pab.2026.10096 Published online by Cambridge University Press

hypsodonty, a fact that is only revealed through careful, phylogenetically informed analysis.

Conclusion

Over the last 100 years the story of equid evolution has been continually revised. A more complex branching phylogenetic understanding of equid evolutionary relationships has mostly replaced the early orthogenetic narrative (Marsh, 1879; Gidley and Osborn 1907; Matthew 1926, 1930; Stirton 1940; Simpson 1951; MacFadden 1994). Likewise, further explorations of equid evolution have revealed that presumed linear transitions in equid morphology and ecology are actually more complex than previously assumed. For example, digit reduction is actually best thought of as a continuous trait, rather than a discrete transitions between monodactyl and tridactyl conditions (McHorse et al. 2017). Similarly, other lines of evidence such as microwear (Semprebon et al. 2016) and isotopic analysis (MacFadden et al. 1999) have revealed that, in many cases, hypsodont equids were not exclusively grazers and that hypsodonty may have allowed for increased dietary flexibility, rather than specialization (Feranec 2003, 2007; Mihlbachler et al. 2011). Undoubtedly, continued study and development of new methodologies will continue to elucidate evolutionary patterns within the group. Our analysis serves as another line in the ever-evolving story of equid evolution, the trend of which seems to be away from simple narrative and toward ever-increasing complexity.

Acknowledgments. We would like to thank A.L.W.'s graduate committee (D. Jablonski, M. Foote, M. Webster, and Z. X. Luo), L. Weaver, C. Badgley, M. Zelditch, and members of the Slater and Webster labs for providing thoughtful discussion and feedback. We would like to acknowledge the contributions of the collections staff and curators at the American Museum of Natural History (J. Meng, J. Galkin, and R. O'Leary), Natural History Museum of Los Angeles County Museum (S. A. McLeod and X. Wang), University of Nebraska State Museum (R. Secord and G. Corner), Smithsonian National Museum of Natural History (H. Little, N. Pyenson, and A. Millhouse), and Field Museum (K. Angielczyk, B. Simpson, A. Ferguson, and L. Heaney) in facilitating access to the specimens in their care. The authors would also like to extend a special thank you to K. Behrensmeyer for serving as A.L.W.'s predoctoral fellowship mentor at the Smithsonian. Financial support was provided by a Big Ten Academic Alliance Smithsonian Institution Predoctoral Fellowship, Natural History Museum of Los Angeles County Student Collections Study Award, Hinds Fund award, and support from the Gerhley Fund and the Broc Kokesh Memorial Fund for the De-extinction of the Stellar's Seacow to A.L.W. Access to TNT was provided by the Willi Hennig Society. Declaration of use of Artificial Intelligence (AI): We used ChatGPT (Open AI) to assist with aspects of the project: to brainstorm potential titles for the paper, for researching the function of the nasal diverticulum and Flehmen response in equids (ChatGPT 4.5, accessed 5 March 2025), to generate code for some of the analyses presented here (e.g., form space analysis) (ChatGPT5, accessed 1 September 2025), and to format citations (ChatGPT5, accessed 23 October 2025). The authors critically reviewed all outputs before implementing them in the research.

Competing Interests. The authors have no competing interests to declare.

Data Availability Statement. Data and code are available via Dryad and Zenodo: https://doi.org/10.5061/dryad.crjdfn3g3, https://doi.org/10.5281/zenodo.18635760. 3D morphological data are available on Morphosource, Project ID 000715259: https://www.morphosource.org/projects/000715259?locale=en.

Literature Cited

Adams, D. C., and E. Otárola-Castillo. 2013. geomorph: an R package for the collection and analysis of geometric morphometric shape data. *Methods in Ecology and Evolution* **4**:393–399.

Adams, D. C., M. L. Collyer, A. Kaliontzopoulou, and E. K. Baken. 2023. geomorph: software for geometric morphometric analyses, R package version 4.0.6. https://cran.r-project.org/package=geomorph (accessed 23 September 2025).

Bai, B., Y.-Q. Wang, and J. Meng. 2018. The divergence and dispersal of early perissodactyls as evidenced by early Eocene equids from Asia. *Communications Biology* **1**:1–10.

Baken, E. K., M. L. Collyer, A. Kaliontzopoulou, and D. C. Adams. 2021. geomorph v4.0 and gmShiny: enhanced analytics and a new graphical interface for a comprehensive morphometric experience. *Methods in Ecology and Evolution* **12**:2355–2363.

Barrón-Ortiz, C. I., L. S. Avilla, C. N. Jass, V. M. Bravo-Cuevas, H. Machado, and D. Mothé. 2019. What is *Equus*? Reconciling taxonomy and phylogenetic analyses. *Frontiers in Ecology and Evolution* **7**:343.

Baum, B. R. 1992. Combining trees as a way of combining data sets for phylogenetic inference, and the desirability of combining gene trees. *Taxon* **41**:3–10.

Bennett, D. K. 1980. Stripes do not a zebra make, part I: a cladistic analysis of Equus. *Systematic Zoology* **29**:272–287.

Bibi, F., and J. Tyler. 2022. Evolution of the bovid cranium: morphological diversification under allometric constraint. *Communications Biology* **5**:69.

Bouckaert, R., J. Heled, D. Kühnert, T. Vaughan, C.-H. Wu, D. Xie, M. A. Suchard, A. Rambaut, and A. J. Drummond. 2014. BEAST 2: a software platform for Bayesian evolutionary analysis. *PLoS Computational Biology* **10**: e1003537.

Bright, J. A., J. Marugán-Lobón, S. N. Cobb, and E. J. Rayfield. 2016. The shapes of bird beaks are highly controlled by nondietary factors. *Proceedings of the National Academy of Sciences USA* **113**:5352–5357.

Budras, K. D., W. O. Sack, S. Rock, A. Horowitz, and R. Berg. 2012. *Anatomy of the horse*. Schlütersche, Hannover.

Cantalapiedra, J. L., J. L. Prado, M. Hernández Fernández, and M. T. Alberdi. 2017. Decoupled ecomorphological evolution and diversification in Neogene–Quaternary horses. *Science* **355**:627–630.

Cardini, A., D. Polly, R. Dawson, and N. Milne. 2015. Why the long face? Kangaroos and wallabies follow the same 'rule' of cranial evolutionary allometry (CREA) as placentals. *Evolutionary Biology* **42**:169–176.

Cardini, A. 2019. Craniofacial allometry is a rule in evolutionary radiations of placentals. *Evolutionary Biology* **46**:239–248.

Cardini, A., and P. D. Polly. 2013. Larger mammals have longer faces because of size-related constraints on skull form. *Nature Communications* **4**:2458.

Cirilli, O., L. Pandolfi, L. Rook, and R. L. Bernor. 2021. Evolution of Old World *Equus* and origin of the zebra–ass clade. *Scientific Reports* **11**:10156.

Clavel, J., G. Escarguel, and G. Merceron. 2015. mvMORPH: an R package for fitting multivariate evolutionary models to morphometric data. *Methods in Ecology and Evolution* **6**:1311–1319.

Crowell-Davis, S., and K. A. Houpt. 1985. The ontogeny of flehmen in horses. *Animal Behaviour* **33**:739–745.

Danilo, L., J. A. Remy, M. Vianey-Liaud, B. Marandat, J. Sudre, and F. Lihoreau. 2013. A new Eocene locality in southern France sheds light on the basal radiation of Palaeotheriidae (Mammalia, Perissodactyla, Equoidea). *Journal of Vertebrate Paleontology* **33**:195–215.

Drummond, A. J., M. A. Suchard, D. Xie, and A. Rambaut. 2012. Bayesian phylogenetics with BEAUti and the BEAST 1.7. *Molecular Biology and Evolution* **29**:1969–1973.

Emerson, S. B., and D. M. Bramble. 1993. Scaling, allometry, and skull design. Pp. 384–421 *in* J. Hanken and B. K. Hall, eds. The skull, Vol. **3**. *Functional and evolutionary mechanisms*. University of Chicago Press, Chicago.

Estes, R. D. 1972. The role of the vomeronasal organ in mammalian reproduction. *Extrait de Mammalia* **36**:315–341.

Evander, R. L. 1989. Phylogeny of the family Equidae. Pp. 109–127 *in* D. R. Prothero and R. M. Schoch, eds. *The evolution of perissodactyls*. Oxford University Press, New York.

Famoso, N. A., E. B. Davis, R. S. Feranec, S. S. B. Hopkins, and S. A. Price. 2016. Are hypsodonty and occlusal enamel complexity evolutionarily correlated in ungulates? *Journal of Mammalian Evolution* **23**:43–47.

Felsenstein, J. 1985. Phylogenies and the comparative method. *American Naturalist* **125**:1–15.

https://doi.org/10.1017/pab.2026.10096 Published online by Cambridge University Press

Feranec, R. S. 2003. Stable isotopes, hypsodonty, and the paleodiet of *Hemiauchenia* (Mammalia: Camelidae): a morphological specialization creating ecological generalization. *Paleobiology* **29**:230–242.

Feranec, R. S. 2007. Ecological generalization during adaptive radiation: evidence from Neogene mammals. *Evolutionary Ecology Research* **9**:555–577.

Foote, M. 1997. The evolution of morphological diversity. *Annual Review of Ecology and Systematics* **28**:129–152.

Foote, M. 1996. Models of morphological diversification. Pp. 62–86 *in* D. Jablonski, D. H. Erwin, and J. H. Lipps, eds. *Evolutionary paleobiology*. University of Chicago Press, Chicago.

Froehlich, D. J. 2002. Quo vadis eohippus? The systematics and taxonomy of the early Eocene equids (Perissodactyla). *Zoological Journal of the Linnean Society* **134**:141–256.

Gavryushkina, A., T. A. Heath, D. T. Ksepka, T. Stadler, D. Welch, and A. J. Drummond. 2017. Bayesian total-evidence dating reveals the recent crown radiation of penguins. *Systematic Biology* **66**:57–73.

Giannini, N.P., V. Segura, M. I. Giannini, and D. Flores. 2010. A quantitative approach to the cranial ontogeny of the puma. *Mammalian Biology* **75**: 547–554

Gidley, J. W., and H. F. Osborn. 1907. Revision of the Miocene and Pliocene Equidae of North America. *Bulletin of the American Museum of Natural History* **23**:865–934.

Goloboff, P. A., and M. E. Morales. 2023. TNT version 1.6, with a graphical interface for macOS and Linux, including new routines in parallel. *Cladistics* **39**:144–153.

Goswami, A., and P. D. Polly. 2010. Methods for studying morphological integration and modularity. *Paleontological Society Papers* **16**:213–243.

Goswami, A., E. Noirault, E. J. Coombs, J. Clavel, A.-C. Fabre, T. J. Halliday, M. Churchill, et al. 2022. Attenuated evolution of mammals through the Cenozoic. *Science* **378**:377–383.

Gould, S. J. 1985. *Ontogeny and phylogeny*. Harvard University Press, Cambridge, Mass.

Gould, S. J., and R. C. Lewontin. 1979. The spandrels of San Marco and the Panglossian paradigm: a critique of the adaptationist programme. *Proceedings of the Royal Society B* **205**:581–598.

Grafen, A. 1989. The phylogenetic regression. *Philosophical Transactions of the Royal Society B* **326**:119–157.

Gregory, W. K. 1920. Studies in comparative myology and osteology. No. 5: On the anatomy of the preorbital fossae of Equidae and other ungulates. *Bulletin of the American Museum of Natural History* **42**:265–284.

Hallgrímsson, B., J. J. Brown, A. F. Ford-Hutchinson, H. D. Sheets, M. L. Zelditch, and F. R. Jirik. 2006. The brachymorph mouse and the developmental-genetic basis for canalization and morphological integration. *Evolution and Development* **8**:61–73.

Hansen, T. F. 1997. Stabilizing selection and the comparative analysis of adaptation. *Evolution* **51**:1341–1351.

Heath, T. A., J. P. Huelsenbeck, and T. Stadler. 2014. The fossilized birth–death process for coherent calibration of divergence-time estimates. *Proceedings of the National Academy of Sciences USA* **111**:E2957–E2966.

Heck, L., L. A. Wilson, A. Evin, M. Stange, and M. R. Sánchez-Villagra. 2018. Shape variation and modularity of skull and teeth in domesticated horses and wild equids. *Frontiers in Zoology* **15**:1–17.

Heck, L., M. R. Sanchez-Villagra, and M. Stange. 2019. Why the long face? Comparative shape analysis of miniature, pony, and other horse skulls reveals changes in ontogenetic growth. *PeerJ* **7**:e7678.

Heintzman, P. D., G. D. Zazula, R. D. MacPhee, E. Scott, J. A. Cahill, B. K. McHorse, J. D. Kapp, et al. 2017. A new genus of horse from Pleistocene North America. *eLife* **6**:e29944.

Hulbert, R. C., Jr. 1989. Phylogenetic interrelationships and evolution of North American late Neogene Equinae. Pp. 176–194 *in* D. R. Prothero and R. M. Schoch, eds. *The evolution of perissodactyls*. Oxford University Press, New York.

Hulbert, R. C., and B. J. MacFadden. 1991. Morphological transformation and cladogenesis at the base of the adaptive radiation of Miocene hypsodont horses. *American Museum Novitates* **3000**:1–61.

Jablonski, D. 2017a. Approaches to macroevolution: 1. General concepts and origin of variation. *Evolutionary Biology* **44**:427–450.

Jablonski, D. 2017b. Approaches to macroevolution: 2. Sorting of variation, some overarching issues, and general conclusions. *Evolutionary Biology* **44**: 451–475.

Jablonski, D. 2020. Developmental bias, macroevolution, and the fossil record. *Evolution and Development* **22**:103–125.

Janis, C. 2007. The horse series. Pp. 251–280 *in* B. Regal, ed. *Icons of evolution*. Greenwood Press, Westport, Conn.

Jombart, T., M. Kendall, J. Almagro-Garcia, and C. Colijn. 2017. TREESPACE: statistical exploration of landscapes of phylogenetic trees. *Molecular Ecology Resources* **17**:1385–1392.

Kelly, T. S. 1998. New middle Miocene equid crania from California and their implications for the phylogeny of the Equini. *Natural History Museum of Los Angeles County, Contributions in Science* **473**:1–43.

Klingenberg, C. P. 2014. Studying morphological integration and modularity at multiple levels: concepts and analysis. *Philosophical Transactions of the Royal Society B* **369**:20130249.

Krone, I. W., C. F. Kammerer, and K. D. Angielczyk. 2019. The many faces of synapsid cranial allometry. *Paleobiology* **45**:531–545.

Le Verger, K., L. Hautier, J. Bardin, S. Gerber, F. Delsuc, and G. Billet. 2020. Ontogenetic and static allometry in the skull and cranial units of nine-banded armadillos (Cingulata: Dasypodidae: *Dasypus novemcinctus*). *Biological Journal of the Linnean Society*. **131**:673–698.

Linde-Medina, M. 2016. Testing the cranial evolutionary allometric "rule" in Galliformes. *Journal of Evolutionary Biology* **29**:1873–1878.

Lloyd, G., D. Bapst, M. Friedman, and K. Davis. 2016. Probabilistic divergence time estimation without branch lengths: dating the origins of dinosaurs, avian flight and crown birds. *Biology Letters* **12**:20160609.

Lloyd, G. T. 2015. metatree: generating meta-analytical phylogenies. R package version 0.1. GitHub. https://github.com/graemetlloyd/metatree (accessed 23 September 2025).

Lloyd, G. T., and G. J. Slater. 2021. A total-group phylogenetic metatree for Cetacea and the importance of fossil data in diversification analyses. *Systematic Biology* **70**:922–939.

MacFadden, B. J. 1994. *Fossil horses: systematics, paleobiology, and evolution of the family Equidae*. Cambridge University Press, Cambridge.

MacFadden, B. J., and M. F. Skinner. 1982. Hipparion horses and modern phylogenetic interpretation: comments on Forsten's view of Cormohipparion. *Journal of Paleontology* **56**:1336–1342.

MacFadden, B. J., N. Solounias, and T. E. Cerling. 1999. Ancient diets, ecology, and extinction of 5-million-year-old horses from Florida. *Science* **283**:824–827.

Marcy, A. E., T. Guillerme, E. Sherratt, K. C. Rowe, M. J. Phillips, and V. Weisbecker. 2020. Australian rodents reveal conserved cranial evolutionary allometry across 10 million years of murid evolution. *American Naturalist* **196**:755–768.

Marroig, G., and J. M. Cheverud. 2005. Size as a line of least evolutionary resistance: diet and adaptive morphological radiation in New World monkeys. *Evolution* **59**:1128–1142.

Marsh, O. C. 1879. Polydactyl horses, recent and extinct. *American Journal of Science* **17**:499–505.

Martin, R. D., M. Genoud, and C. K. Hemelrijk. 2005. Problems of allometric scaling analysis: examples from mammalian reproductive biology. *Journal of Experimental Biology* **208**:1731–1747.

Matthew, W. 1930. The pattern of evolution. *Scientific American* **143**:192–196.

Matthew, W. D. 1926. The evolution of the horse: a record and its interpretation. *Quarterly Review of Biology* **1**:139–185.

McHorse, B. K., A. A. Biewener, and S. E. Pierce. 2017. Mechanics of evolutionary digit reduction in fossil horses (Equidae). *Proceedings of the Royal Society B* **284**:20171174.

Meloro, C., and G. J. Slater. 2012. Covariation in the skull modules of cats: the challenge of growing saber-like canines. *Journal of Vertebrate Paleontology* **32**:677–685.

Mihlbachler, M. C., F. Rivals, N. Solounias, and G. M. Semprebon. 2011. Dietary change and evolution of horses in North America. *Science* **331**: 1178–1181.

Mitchell, D. R., E. Sherratt, and V. Weisbecker. 2024. Facing the facts: adaptive trade-offs along body size ranges determine mammalian craniofacial scaling. *Biological Reviews* **99**:496–524.

https://doi.org/10.1017/pab.2026.10096 Published online by Cambridge University Press

O'Higgins, P., and M. Collard. 2002. Sexual dimorphism and facial growth in papionin monkeys. *Journal of Zoology* **257**:255–272

O'Sullivan, J. A. 2002. *Paleobiology of* Archaeohippus *(Mammalia; Equidae): a three -toed horse from the Oligocene–Miocene of North America*. Ph.D. dissertation. University of Florida, Gainesville. https://www.proquest.com/docview/275918031?fromopenview=true&pq-origsite=gscholar&sourcetype=Dissertations%20&%20Theses.

Pagnac, D. 2006. *Scaphohippus*, a new genus of horse (Mammalia: Equidae) from the Barstow Formation of California. *Journal of Mammalian Evolution* **13**:37–61.

Parker, A. K., B. K. McHorse, and S. E. Pierce. 2018. Niche modeling reveals lack of broad-scale habitat partitioning in extinct horses of North America. *Palaeogeography, Palaeoclimatology, Palaeoecology* **511**:103–118.

Prado, J. L., and M. T. Alberdi. 1996. A cladistic analysis of the horses of the tribe Equini. *Palaeontology* **39**:663–680.

Radinsky, L. 1984. Ontogeny and phylogeny in horse skull evolution. *Evolution* **38**:1–15.

Radinsky, L. 1985. Approaches in evolutionary morphology: a search for patterns. *Annual Review of Ecology and Systematics* **16**:1–14.

Ragan, M. A. 1992a. Matrix representation in reconstructing phylogenetic relationships among the eukaryotes. *Biosystems* **28**:47–55.

Ragan, M. A. 1992b. Phylogenetic inference based on matrix representation of trees. *Molecular Phylogenetics and Evolution* **1**:53–58.

Raup, D. M., and S. J. Gould. 1974. Stochastic simulation and evolution of morphology—towards a nomothetic paleontology. *Systematic Biology* **23**:305–322.

Reeve, E., and P. Murray. 1942. Evolution in the horse's skull. *Nature* **150**:402–403.

Revell, L. J. 2010. Phylogenetic signal and linear regression on species data. *Methods in Ecology and Evolution* **1**:319–329.

Rhoda, D. P., A. Haber, and K. D. Angielczyk. 2023. Diversification of the ruminant skull along an evolutionary line of least resistance. *Science Advances* **9**:eade8929.

Richardson, W., N. M. Morales-García, J. Damuth, S. Singh, and C. M. Janis. 2024. Why the short face? The face lengths of sthenurine kangaroos scale with negative allometry. *Journal of Vertebrate Paleontology* **43**:e2336145.

Robb, R. C. 1935. A study of mutations in evolution. I. *Evolution in the equine skull.* Journal of Genetics **31**:39–46.

Rose, K. D., L. T. Holbrook, R. S. Rana, K. Kumar, K. E. Jones, H. E. Ahrens, P. Missiaen, A. Sahni, and T. Smith. 2014. Early Eocene fossils suggest that the mammalian order Perissodactyla originated in India. *Nature Communications* **5**:5570.

Salamanca-Carreño, A., P. M. Parés-Casanova, R. A. Crosby-Granados, M. Vélez-Terranova, and J. Benítez-Molano. 2023. Basicranial modular organization: a study in the Araucanian horse of Colombia. *Veterinary Sciences* **10**:255.

Salazar-Ciudad, I. 2021. Why call it developmental bias when it is just development? *Biology Direct* **16**:1–13.

Schlager, S. 2017. Morpho and Rvcg—shape analysis in R. Pp. 217–256 *in* G. Zheng, S. Li, and G. Szekely, eds. *Statistical shape and deformation analysis: methods, implementation and applications*. Elsevier, Amsterdam.

Schlager, S., A. Profico, F. Di Vincenzo, and G. Manzi. 2018. Retrodeformation of fossil specimens based on 3D bilateral semi-landmarks: implementation in the R package Morpho. *PLoS ONE* **13**:e0194073.

Schluter, D. 1996. Adaptive radiation along genetic lines of least resistance. *Evolution* **50**:1766–1774.

Semprebon, G. M., F. Rivals, N. Solounias, and R. C. Hulbert Jr. 2016. Paleodietary reconstruction of fossil horses from the Eocene through Pleistocene of North America. *Palaeogeography, Palaeoclimatology, Palaeoecology* **442**:110–127.

Simpson, G. G. 1944. *Tempo and mode in evolution*. Columbia University Press, New York.

Simpson, G. G. 1951. *Horses: the story of the horse family in the modern world and through sixty million years of history*. Oxford University Press, Oxford.

Simpson, G. G. 1953. *The major features of evolution*. Columbia University Press, New York.

Slater, G. J., and B. Van Valkenburgh. 2008. Long in the tooth: evolution of sabertooth cat cranial shape. *Paleobiology* **34**:403–419.

Stirton, R. A. 1940. Phylogeny of North American Equidae. *University of California Publications, Bulletin of the Department of Geological Sciences* **25**:165–198.

Strömberg, C. A. 2006. Evolution of hypsodonty in equids: testing a hypothesis of adaptation. *Paleobiology* **32**:236–258.

Symonds, M. R. E., and S. P. Blomberg. 2014. A primer on phylogenetic generalised least squares. Pp. 105–130 *in* L. Z. Garamszegi, ed. *Modern phylogenetic comparative methods and their application in evolutionary biology: concepts and practice*. Springer, Berlin.

Tamagnini, D., C. Meloro, and A. Cardini, A. 2017. Anyone with a long-face? Craniofacial evolutionary allometry (CREA) in a family of short-faced mammals, the Felidae. *Evolutionary Biology* **44**:476–495.

Tamagnini, D., D. Canestrelli, C. Meloro, P. Raia, and L. Maiorano. 2021. New avenues for old travellers: phenotypic evolutionary trends meet morphodynamics, and both enter the global change biology era. *Evolutionary Biology* **48**:379–393.

Tamagnini, D., M. Michaud, C. Meloro, P. Raia, L. Soibelzon, P. S. Tambusso, L. Varela, and L. Maiorano. 2023. Conical and sabertoothed cats as an exception to craniofacial evolutionary allometry. *Scientific Reports* **13**:13571.

Uyeda, J. C., R. Zenil-Ferguson, and M. W. Pennell. 2018. Rethinking phylogenetic comparative methods. *Systematic Biology* **67**:1091–1109.

Wayne, R. K. 1986. Cranial morphology of domestic and wild canids: the influence of development on morphological change. *Evolution* **40**:243–261.

Webster, M., and H. D. Sheets. 2010. A practical introduction to landmark-based geometric morphometrics. *Paleontological Society Papers* **16**:163–188.

Wing, S. L. 1998. Tertiary vegetation of North America as a context for mammalian evolution. Pp. 37–65 *in* C. M. Janis, K. M. Scott, and L. L. Jacobs, eds. *Evolution of tertiary mammals of North America*, Vol. **1**. *Terrestrial carnivores, ungulates, and ungulate like mammals.* Cambridge University Press, Cambridge.

Wisniewski, A. L., G. T. Lloyd, and G. J. Slater. 2022. Extant species fail to estimate ancestral geographical ranges at older nodes in primate phylogeny. *Proceedings of the Royal Society B* **289**:20212535.

Woodburne, M. O. 2007. Phyletic diversification of the *Cormohipparion occidentale* complex (Mammalia; Perissodactyla, Equidae), late Miocene, North America, and the origin of the Old World *Hippotherium* datum. *Bulletin of the American Museum of Natural History* **306**:1–138.

Zelditch, M. L., and D. L. Swiderski. 2023. The predictable complexity of evolutionary allometry. *Evolutionary Biology* **50**:56–77.

https://doi.org/10.1017/pab.2026.10096 Published online by Cambridge University Press